

# Hybrid $\text{Fe}_3\text{O}_4 / \text{GaAs}(100)$ structure for spintronics

Cite as: J. Appl. Phys. **97**, 10C313 (2005); <https://doi.org/10.1063/1.1857432>

Published Online: 04 May 2005

Y. X. Lu, J. S. Claydon, E. Ahmad, Y. B. Xu, M. Ali, B. J. Hickey, S. M. Thompson, J. A. D. Matthew, and K. Wilson



View Online



Export Citation

## ARTICLES YOU MAY BE INTERESTED IN

[Fast x-ray spectroscopy study of ethene on clean and  \$\text{SO}\_4\$  precovered Pt{111}](#)

Journal of Vacuum Science & Technology A **21**, 563 (2003); <https://doi.org/10.1116/1.1559923>

[Spin and orbital moments of nanoscale  \$\text{Fe}\_3\text{O}\_4\$  epitaxial thin film on  \$\text{MgO}/\text{GaAs}\(100\)\$](#)

Applied Physics Letters **104**, 142407 (2014); <https://doi.org/10.1063/1.4871001>

[Epitaxial growth and magnetic properties of ultrathin iron oxide films on  \$\text{BaTiO}\_3\(001\)\$](#)

Journal of Applied Physics **114**, 113901 (2013); <https://doi.org/10.1063/1.4821259>

### Ultra High Performance SDD Detectors



See all our XRF Solutions

## Hybrid Fe<sub>3</sub>O<sub>4</sub>/GaAs(100) structure for spintronics

Y. X. Lu, J. S. Claydon, E. Ahmad, and Y. B. Xu<sup>a)</sup>

*Spintronics Laboratory, Department of Electronics, University of York, York, YO10 5DD, United Kingdom*

M. Ali and B. J. Hickey

*Department of Physics and Astronomy, E. C. Stoner Laboratory, University of Leeds, Leeds, LS2 9JT, United Kingdom*

S. M. Thompson and J. A. D. Matthew

*Department of Physics, University of York, York, YO10 5DD, United Kingdom*

K. Wilson

*Department of Chemistry, University of York, York, YO10 5DD, United Kingdom*

(Presented on 8 November 2004; published online 4 May 2005)

Fe<sub>3</sub>O<sub>4</sub>/GaAs hybrid structures have been studied using reflection high-energy electron diffraction (RHEED), x-ray photoelectron spectroscopy (XPS), x-ray magnetic circular dichroism (XMCD), and low-temperature vibrating-sample magnetometry (VSM). The samples were prepared by oxidizing epitaxial Fe thin films in a partial pressure of  $5 \times 10^{-5}$  mbar of oxygen at 500 K for 180 s. Clear RHEED patterns were observed, suggesting the epitaxial growth of Fe oxides with a cubic structure. The XPS spectra show that the oxides were Fe<sub>3</sub>O<sub>4</sub> rather than  $\gamma$ -Fe<sub>2</sub>O<sub>3</sub>, as there were no shake-up satellites between the two Fe 2*p* peaks. This was further confirmed by the XMCD measurements, which show ferromagnetic coupling between the Fe cations, with no evidence of intermixing at the interface. The VSM measurements show that the films have a magnetic uniaxial anisotropy and a “quick” saturation property, with the easy axes along the [0 $\bar{1}1$ ] direction. This detailed study offers further insight into the structure, interface, and magnetic properties of this hybrid Fe<sub>3</sub>O<sub>4</sub>/GaAs(100) structure as a promising system for spintronic application. © 2005 American Institute of Physics. [DOI: 10.1063/1.1857432]

### I. INTRODUCTION

Magnetic oxides, such as Fe<sub>3</sub>O<sub>4</sub> and CrO<sub>2</sub>, have drawn intensive attention due to their half-metallicity and potential application in spintronics.<sup>1</sup> The iron oxide, Fe<sub>3</sub>O<sub>4</sub>, known as magnetite, has been prepared on Al<sub>2</sub>O<sub>3</sub>,<sup>2</sup> MgO,<sup>2-5</sup> and Pt (Ref. 6) substrates. But to integrate with the industry for spintronic application, the preparation of high-quality Fe<sub>3</sub>O<sub>4</sub> on semiconductors, such as GaAs, is essential. At the same time, the Fe<sub>3</sub>O<sub>4</sub> films grown by simultaneous oxidation upon evaporation, or dc reactive sputtering, have shown unexpected magnetic properties, such as superparamagnetism, remaining unsaturated even in the extra field as large as 70 kOe.<sup>2</sup> This slow saturation behavior has been attributed to the antiphase boundaries (APBs) appearing in samples with inverse spinel structure.<sup>4</sup> Does this unfavorable behavior persist for ultrathin Fe<sub>3</sub>O<sub>4</sub>, grown by postgrowth oxidation rather than by simultaneous oxidation? Another subject matter, to be clarified, is the interface and surface composition of the sample. When oxidized, how does the metallic Fe react with oxygen during the oxidation process at the GaAs surface? These problems are important for spin injection and the fundamental understanding of the oxide growth on semiconductors.

Our previous magneto-optical Kerr effect (MOKE) measurements of the Fe<sub>3</sub>O<sub>4</sub>/GaAs(100) hybrid structures have demonstrated the magnetic behavior, which is uniaxial in

nature.<sup>7</sup> In this paper, we present a detailed study of the Fe<sub>3</sub>O<sub>4</sub>/GaAs(100) hybrid structure using reflection high-energy electron diffraction (RHEED), x-ray photoelectron spectroscopy (XPS), x-ray magnetic circular dichroism (XMCD), and low-temperature vibrating-sample magnetometry (VSM). The VSM measurement demonstrated that the slow saturation behavior is clearly absent. With XPS and XMCD, we provide further insight into the surface and interface characteristics of these structures.

### II. EXPERIMENT

The magnetite samples were prepared by postgrowth oxidation of the pregrown epitaxial Fe on GaAs(100). The substrates were first chemically etched in a solution of H<sub>2</sub>SO<sub>4</sub>:H<sub>2</sub>O<sub>2</sub>:H<sub>2</sub>O (4:1:1) for 30 s and rinsed in de-ionized water. After this the substrate was transferred to the growth/oxidation chamber, where a thermal annealing at 830 K for 30 min was performed, prior to growth. The Fe was held in a crucible and heated by an electron beam. The Fe growth rate was set to 2 Å/min, monitored by a quartz microbalance and the thicknesses were kept below 3 nm. The as-grown samples were then oxidized in an O<sub>2</sub> environment of  $5 \times 10^{-5}$  mbar at 500 K for 180 s. During the growth phase, RHEED measurements were made to monitor the crystal structure and morphology of the samples. The diffraction images were recorded with a charge-coupled device (CCD) camera.

<sup>a)</sup>Electronic mail: yx2@york.ac.uk

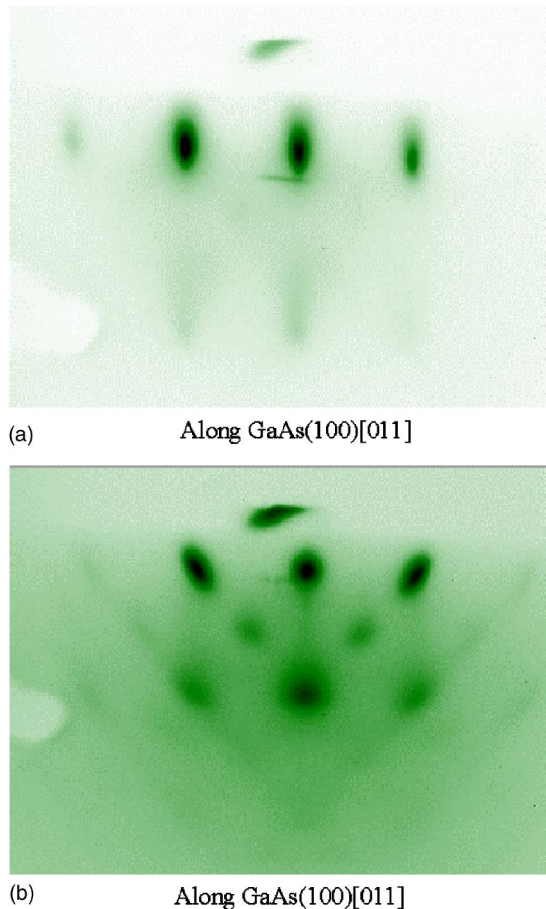


FIG. 1. RHEED images of the 3-nm Fe (a) and  $\text{Fe}_3\text{O}_4$  (b) on GaAs(100) taken along the GaAs[011] direction. The high voltage of the RHEED gun is set to 10.0 kV.

When the oxide reaches a stable phase, showing no change in the RHEED pattern on further exposure to oxygen, the samples were taken out from the UHV chamber and exposed to air without any capping layer. VSM and MOKE measurements were carried out to detect the magnetic properties. Following this XPS measurements were performed with  $\text{Mg } K\alpha$  radiation. XMCD measurements were carried out in station 1.1 of the Synchrotron Radiation Source at Daresbury Laboratory (U. K.). The resulting current output from the sample was measured in total electron yield mode as a function of the photon energy. The dichroism was obtained as the difference spectrum,  $I^+ - I^-$ , achieved by reversing the direction of the applied magnetic field at fixed polarization.

### III. RESULTS AND DISCUSSION

The RHEED pattern of the 3-nm epitaxial Fe on GaAs(100) along the [011] direction is shown in Fig. 1(a). The RHEED pattern along the  $[0\bar{1}1]$  direction (not shown here) is the same as Fig. 1(a), indicating a fourfold symmetry in the Fe crystal structure, consistent with the body-centered-cubic (bcc) structure. Shown in Fig. 1(b) is the RHEED pattern of the Fe oxide obtained along the GaAs(100)[011] direction. Simple calculation of the lattice parameter, according to the diffraction spots and comparison of the pat-

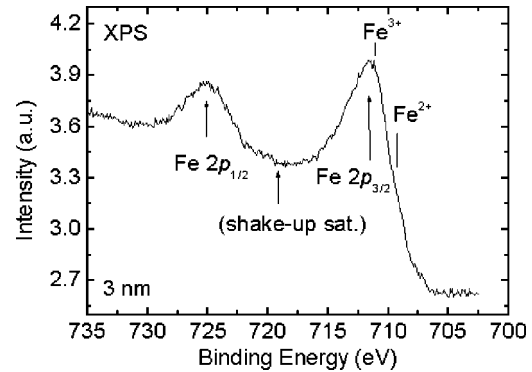


FIG. 2. The XPS core-level peaks of the 3-nm oxidized Fe. The Fe  $2p_{1/2}$  and Fe  $2p_{3/2}$  peaks are indicated by the arrows. Between these two  $2p$  peaks, there is no satellite, which is the characteristics of  $\text{Fe}_2\text{O}_3$ , at the energy position indicated.

tern with other reported RHEED images, is consistent with a  $\text{Fe}_3\text{O}_4$  crystal structure.<sup>5</sup> However, the crystal structure of  $\gamma\text{-Fe}_2\text{O}_3$  is very similar to the  $\text{Fe}_3\text{O}_4$  and additional analysis was performed to examine the composition of the sample.

Verwey transition is believed to be a characteristic of the bulk  $\text{Fe}_3\text{O}_4$ . This is because of the freezing of the hopping electron between Fe cations upon cooling of the sample to around 120 K in the bulk  $\text{Fe}_3\text{O}_4$  material. However, for ultrathin  $\text{Fe}_3\text{O}_4$  films, the Verwey transition was found to be absent.<sup>8,9</sup> Therefore, rather than adopting this transition to characterize the oxides, we applied XPS, x-ray absorption spectroscopy (XAS), and XMCD to clarify the chemical states of the samples.

To study the surface composition of the structure, a 3-nm sample was measured with XPS and the Fe  $2p$  core-level peaks are shown in Fig. 2. The main peak is visible at an energy of 711.0 eV, consistent with other reports.<sup>10</sup> The peaks are broader compared to the atomic Fe peaks. This can be explained by referring to the different chemical states of Fe cations presented in the sample. From the spectra another contributor can be identified, as marked in Fig. 2, with an energy of about 0.6 eV below that of the main peak. This peak is caused by the  $\text{Fe}^{2+}$  cations in the sample.<sup>10</sup> No shake-up satellite is detected in the spectrum. The shake-up satellite is the fingerprint of  $\text{Fe}_2\text{O}_3$ , and this satellite-free spectrum of the sample excludes the possible presence of  $\gamma\text{-Fe}_2\text{O}_3$ .

The XAS and XMCD measurements of a 2-nm sample are shown in Fig. 3 with an emphasis on the interface and surface of  $\text{Fe}_3\text{O}_4/\text{GaAs}(100)$  structure. In a previous work the  $\text{Fe}_3\text{O}_4/\text{GaAs}(100)$  structure was observed to display macroscopic-ferromagnetic behavior at around 2 nm (nominal thickness), measured by room-temperature MOKE.<sup>7</sup> In inverse spinel structure  $\text{Fe}_3\text{O}_4$  crystal, one-third of all the Fe cations take up all the tetrahedral sites, and another one-third of the Fe cations fill half of the octahedral sites. These two kinds of Fe cations are antiferromagnetically coupled. The rest of the Fe cations inhabit the octahedral site. Here, clearly the contribution from the  $\text{Fe}_{\text{td}}^{3+}$  ( $\text{Fe}^{3+}$  cations at the tetrahedral sites) and  $\text{Fe}_{\text{oh}}^{3+}$  ( $\text{Fe}^{3+}$  cations at the octahedral sites) cancel each other out and the macroscopic ferromagnetism comes from the  $\text{Fe}_{\text{oh}}^{2+}$  cations. The shape of the XMCD spectra for

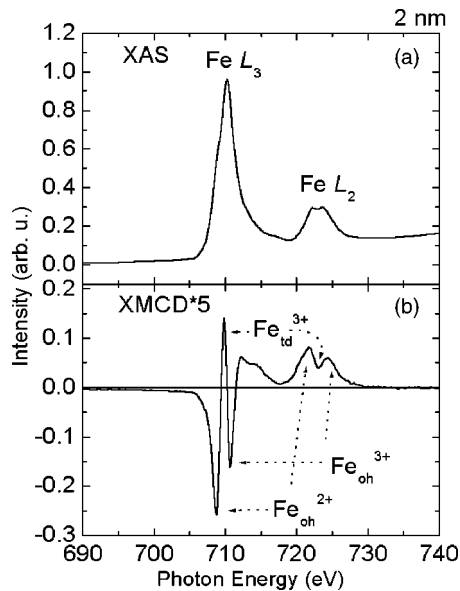


FIG. 3. The XAS (a) and XMCD (b) measurements of the 2-nm  $\text{Fe}_3\text{O}_4/\text{GaAs}(100)$  samples. The  $\text{Fe}_{\text{oh}}^{2+}$ ,  $\text{Fe}_{\text{td}}^{3+}$ , and  $\text{Fe}_{\text{oh}}^{3+}$  peaks in the  $\text{Fe } L_3$  and  $\text{Fe } L_2$  edges are indicated.

the 2-nm sample is almost the same as the spectra obtained from other reports.<sup>11</sup> It was reported previously that at an elevated deposition temperature, Fe on GaAs(100) substrate reacts with As from the substrate and forms a nonmagnetic “dead” layer at the interface. But for the 2-nm sample, the XAS and XMCD spectra showed  $\text{Fe}_3\text{O}_4$  characteristics and no evidence of the presence of any Fe–As compound.

Figure 4 depicts the low-temperature (150 K) VSM measurements of the 3-nm sample along the GaAs(100) [001] and [0 $\bar{1}1$ ] directions. Magnetic uniaxial anisotropy is clearly defined, with a ratio of  $M_r/M_s$  close to 1 and to 0 when the applied magnetic fields were along the [0 $\bar{1}1$ ] and [011] directions, respectively. The coercivity of the sample is around 250 Oe. Interestingly, the sample saturates quickly and the saturation field along the hard axis (the [011] direc-

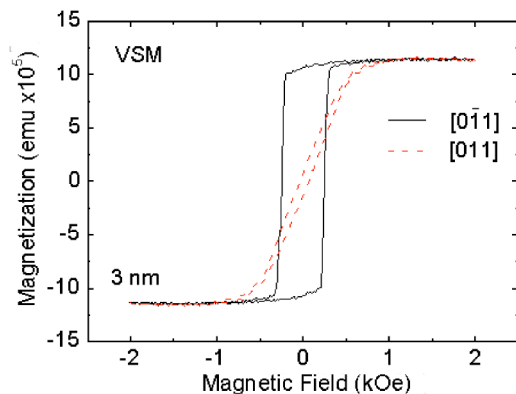


FIG. 4. Low-temperature VSM measurement of the 3-nm sample with magnetic field along the GaAs(100)[011] and [0 $\bar{1}1$ ] directions. The uniaxial magnetic anisotropy can be concluded from the different remnant ratio of the loops along these two directions.

tion of the GaAs) is around 900 Oe, which is greatly reduced compared to what is reported in the literature.<sup>2</sup> We attributed this reduction of saturation field to the decrease of APBs in the samples due to our preparation process. As the sample was prepared by postgrowth oxidation, the  $\text{Fe}_3\text{O}_4$  first nucleates on the Fe surface and then grows. The Fe cations migrate from the Fe/oxide interface through the ionic oxide to the oxide/oxygen surface; the cations are added to the oxide which then thickens. Eventually, the whole ultrathin Fe film becomes oxidized.<sup>12</sup> In this scenario the Fe is quickly oxidized and grows epitaxially on the previously generated  $\text{Fe}_3\text{O}_4$ . While in the simultaneous oxidation, the oxidation might take place before the Fe atoms reach the substrate or the previously deposited oxides. In any event, the substrate or the deposited oxides are always oxygen rich due to the environment. So the APBs would be easy to develop in this simultaneous oxidation. However, in the postgrowth oxidation, the formation of the APBs is suppressed, as suggested by this study.

#### IV. CONCLUSION

The magnetic properties of the surface and the interface of the  $\text{Fe}_3\text{O}_4/\text{GaAs}(100)$  hybrid structure have been investigated. Epitaxial  $\text{Fe}_3\text{O}_4$  has been prepared on GaAs(100) by postgrowth oxidation. The surface of the sample is revealed to be  $\text{Fe}_3\text{O}_4$  rather than  $\text{Fe}_2\text{O}_3$ . The Fe was found to react preferentially with the oxygen, by migration, rather than with As from the substrate. The XPS and XMCD measurements support this conclusion. The VSM loops indicate that the ultrathin  $\text{Fe}_3\text{O}_4$  film unambiguously exhibits a quick saturation behavior with a saturated field of 900 Oe. The  $\text{Fe}_3\text{O}_4/\text{GaAs}(100)$  hybrid structures appear to be a promising candidate for spintronic devices.

#### ACKNOWLEDGMENTS

Financial support from the EPSRC, the White Rose Scholarship, and the Scholarship for Overseas Student from University of York are greatly acknowledged.

<sup>1</sup>J. M. D. Coey and C. L. Chien, MRS Bull. **28**, 720 (2003).

<sup>2</sup>D. T. Margulies, F. T. Parker, F. E. Spada, R. S. Goldman, J. Li, R. Sinclair, and A. E. Berkowitz, Phys. Rev. B **53**, 9175 (1996).

<sup>3</sup>T. Fujii, M. Takano, R. Katano, and Y. Bando, J. Cryst. Growth **99**, 606 (1990).

<sup>4</sup>F. C. Voogt, T. T. M. Palstra, L. Niesen, O. C. Rogojuanu, M. A. James, and T. Hibma, Phys. Rev. B **57**, R8107 (1998).

<sup>5</sup>C. Ruby, J. Fussy, and J.-M. R. Genin, Thin Solid Films **352**, 22 (1999).

<sup>6</sup>W. Weiss and M. Ritter, Phys. Rev. B **59**, 5201 (1999).

<sup>7</sup>Y. X. Lu, J. S. Claydon, Y. B. Xu, D. M. Schofield, and S. M. Thompson, J. Appl. Phys. **95**, 7228 (2004).

<sup>8</sup>W. Eerenstein, T. T. M. Palstra, T. Hibma, and S. Celotto, Phys. Rev. B **66**, 201101(R) (2002).

<sup>9</sup>X. W. Li, A. Gupta, G. Xiao, and G. Q. Gong, J. Appl. Phys. **83**, 7049 (1998).

<sup>10</sup>Y. Gao and S. A. Chambers, J. Cryst. Growth **174**, 446 (1997).

<sup>11</sup>P. Morrall, F. Schedin, G. S. Case, M. F. Thomas, E. Dudzik, G. van der Laan, and G. Thornton, Phys. Rev. B **67**, 214408 (2003).

<sup>12</sup>O. Kubaschewski and B. E. Hopkins, *Oxidation of Metals and Alloys*, 2nd ed. (Butterworths, London, 1967).